Surface temperature and spectral measurements at Santiaguito lava dome, Guatemala

Steve T. M. Sahetapy-Engel, Luke P. Flynn, and Andrew J. L. Harris
HIGP/SOEST, University of Hawai'i, Honolulu, Hawaii, USA

Gregg J. Bluth and William I. Rose
Department of Geological Engineering, Geology and Geophysics, Michigan Technological University, Houghton, Michigan, USA

Otoniel Matias
INSIVUMEH, Guatemala City, Guatemala

Received 4 June 2004; revised 23 July 2004; accepted 20 September 2004; published 13 October 2004.

[1] An infrared thermometer, spectroradiometer and digital video camera were used to observe and document short-term evolution of surface brightness temperature and morphology at Santiaguito lava dome, Guatemala. The thermometer dataset shows 40–70 minute-long cooling cycles, each defined by a cooling curve that is both initiated and terminated by rapid increases in temperature due to regular ash venting. The average cooling rate calculated for each cycle range from 0.9 to 1.6°C/min. We applied a two-component thermal mixture model to the spectroradiometer (0.4–2.5 μm) dataset. The results suggest that the observed surface morphology changed from a cool (120–250°C) crust-dominated surface with high temperature fractures (>900°C) in the first segment of the measurement period to an isothermal surface at moderately high temperature (350–500°C) during the second segment. We attribute the change in the thermal state of the surface to the physical rearrangement of the dome's surface during the most energetic of the ash eruptions. *INDEX TERMS:* 8419 Volcanology: Eruption monitoring (7280); 8414 Volcanology: Eruption mechanisms; 8494 Volcanology: Instruments and techniques. **Citation:** Sahetapy-Engel, S. T. M., L. P. Flynn, A. J. L. Harris, G. J. Bluth, W. I. Rose, and O. Matias (2004), Surface temperature and spectral measurements at Santiaguito lava dome, Guatemala, *Geophys. Res. Lett.*, *31*, L19610, doi:10.1029/2004GL020683.

1. Introduction

[2] Since 1975, the activity at Santiaguito dome complex has included regular short-duration eruptions of ash-rich plumes that typically occur at every 0.5–1 h [*Rose*, 1987]. This has occurred along-side constant low-level degassing coupled with persistent extrusion of lava that has built a ~1.1 km^3 dome complex [*Rose*, 1987; *Harris et al.*, 2002]. Current activity is focused on Caliente vent where lava extrusion has formed a rubbly surface comprised of dacitic lava blocks within a ~300 m wide summit crater. Continuing lava extrusion is evident from the slow-moving active block-lava flows that have extended up to 3.8 km from the vent [*Harris et al.*, 2002]. Periodic vertical ash eruptions continue to occur at intervals of ~5 min to <1 hr from a ~150 m wide ring of vents within the crater [*Bluth et al.*, 2002].

[3] In January 2002, for a ~5 hr period we collected remote thermal infrared temperature and spectral radiance measurements as well as digital video footage of the dome surface within the summit vent, during which ~17 ash eruptions occurred. Our objectives were to observe and record short-term changes in the temperature and morphology of the lava dome surface at a time-scale of seconds and to study how temperature and morphology are affected by the periodic ash eruptions. Our data will provide constraints on initial at-vent time-dependent parameters such as temperature, heat flux and crust coverage, all of which are essential input parameters for methods to extract thermal/mass flux data from satellite images, as well as lava flow models that apply to silicic lava domes and flows [e.g., *Harris et al.*, 2002]. For example, thermal remote sensing studies of lava domes typically assume that the observed surface is composed of one, two or three thermal components to retrieve sub-pixel temperatures [e.g., *Rothery et al.*, 1998; *Oppenheimer*, 1993; *Wooster et al.*, 2000]. Thermal structures derived from our dataset will thus help determine and guide the number of components to best represent lava dome surface at Santiaguito.

2. Data Collection

[4] From 4:22 AM until 8:39 AM on January 11, 2002, continuous brightness temperature measurements were collected using a single-channel (8–14 μm) Raytek IR thermometer at 2 s sampling rate. These are integrated brightness temperatures of surfaces that may or may not be thermally homogenous. They do not represent the absolute temperatures of the surfaces because we did not take into account emissivity or atmospheric effects. Five hundred and ninety radiance spectra were collected at 3 s intervals during two nighttime periods within the Raytek time series between 4:31–4:46 AM and 5:29–5:44 AM, using an Analytical Spectral Devices (ASD) FieldSpec FR narrow-band spectroradiometer. The ASD collects radiant flux in the 0.4–2.5 μm range at a 3–10 nm spectral resolution, producing a continuous spectrum averaged from 10 collected spectra. Each measurement period was

0094-8276/04/2004GL020683$05.00

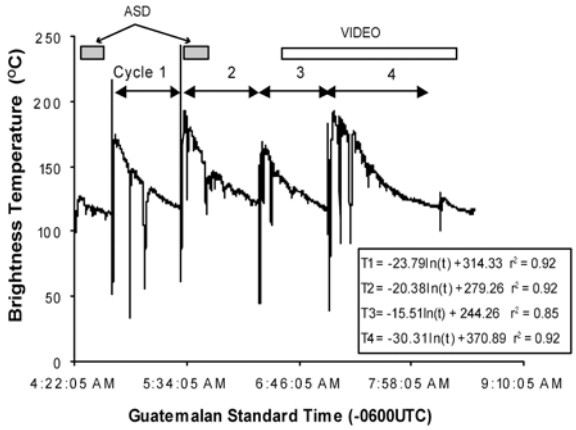

Figure 1. IR thermometer dataset showing the cyclic variations of temperature with time. Four complete cooling cycles are distinguished, designated as cycles 1–4. Best-fit exponential functions for each individual cooling cycle and the r^2 values are shown in the inset.

preceded by a dark current measurement to decrease the amount of noise. All measurements and observations were made from the summit of Volcán Santa Maria (3700 m asl), 2.5 km away from target area (Figure 1). The targeted area is located in the NW sector of the summit crater that was showing the most activity at the initial time of the observation period. Both instruments were equipped with 1° instantaneous field of view (IFOV), equivalent to ~44 m-wide spot (1520 m^2) on the dome surface, which represents ~2.1% of the total area of the summit vent. Both instruments are mounted on heavy-duty tripods secured with rocks at the base to stabilize the IFOV for the observation period. Both also have aiming optical scopes that were used and fine-tuned by looking for maximum radiative response through the IFOV. We acknowledge that the two IFOVs may not be identical which may result in the discrepancy in the area of the dome observed and the derived temperatures between the two instruments. Digital video data were collected from sunrise onwards to give a 2hr-long data set beginning at 6:29AM ending at 8:22AM, overlapping with the latter segment of the IR thermometer dataset.

3. Cooling Cycles

[5] The temperature time series from the IR thermometer reveals cyclic fluctuations in the apparent temperature of the target area (Figure 1). Four complete cooling cycles, between 42 and 72 minutes long, can be distinguished from this dataset. A temperature spike, T_s, ranging from 168–242°C, initiates each cycle and is quickly followed by a 1–3 min period of temperature drop to as low 35°C before recovery to the more typical decaying trend of a cooling curve. Two to three more periods of drastic temperature drops occur in each cycle, at roughly 5-minute intervals. In each cycle the temperature decays exponentially down to an apparent equilibrium end temperature, T_e, of 117–122°C prior to the onset of the next cycle. In cycles 2, 3 and 4 there appear to be periods of small-scale temperature fluctuations (<20°C) from the general cooling trend in the beginning to near the mid-point of each cycle.

[6] Digital video footage is available for the entire duration of cooling cycle #4, allowing linkage of thermal signatures to specific events. Figure 2 provides a summary of the video-observed events during cooling cycle #4. The temperature spike at the onset of the cycle coincides with the relatively energetic ash-rich plume emission event (Figure 2 (mark i)). The dark ash-rich plume dominating the IFOV during the event appears to be the source for the sudden temperature drop, where ash particles within the plume cool very rapidly as air at ambient temperature is entrained in the vertical plume. Two more less-energetic ash plumes also occurred 7 minutes after the first eruption. These plumes erupted approximately ~5 minutes apart with a duration of ~3 min and appear to decrease in relative magnitude successively. Both of these plumes lack initiating high-T spikes, but similar to the first eruption, correspond to periods of low temperature in the Raytek dataset. A ~30 minute-long period of intermittent emission of light-colored gas-rich, low-energy plumes from a vent within the observation area occurred mid-cycle (Figure 2 (mark ii)). This phase can be correlated with the mid-cycle period of small-scale temperature fluctuations in the temperature time-series. Two isolated exhalations of light-colored plumes occur towards the end of the cycle but fail to register any thermal signature in the dataset (Figure 2 (mark iii)). The absence of a thermal signature suggests that the two plumes may be roughly at the same temperatures as the dome surface or that these plumes failed to intersect the IFOV. The cycle then is terminated by an eruption of a darker colored plume with an associated spike, temperature drop and cooling curve pattern.

[7] The general shape of the cooling curve remains relatively constant throughout the cycle for the observed surface. The temperature recovery followed by cooling initiated by each major event suggests that thermal renewal of the surface occurred as a result of the larger of the ash eruptions, where a large fraction of the observed surface is suddenly disturbed. As a result, new hot material may be emplaced, blocks become rotated so that hotter surfaces

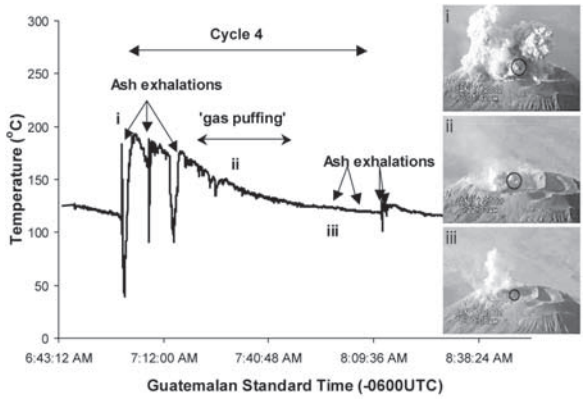

Figure 2. IR temperature measurements for thermal cycle #4 with associated physical events observed from digital video footage. Three captured images show: (i) ash eruption at the initiation of the cycle, (ii) mid-cycle semi continuous gas puffing and (iii) small plumes with no thermal signature. Note the approximate IFOV shown as black circle in the photo sequence.

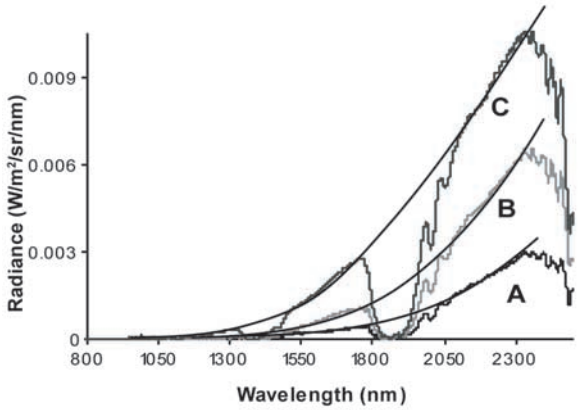

Figure 3. Three representative radiance flux spectrum from segment 1 (A and B) and segment 2 (C). Best-fit curves calculated from our model for each spectrum are shown in solid black curves. All radiance spectra were collected at night to avoid contamination by solar irradiation.

now face up and high temperature cracks form: thus increasing the integrated temperature. Clearly the intermediate and minor events were insufficiently energetic to force such thermal renewal and/or only affected limited areas beyond the measurement area considered. Comprehensive characterization of the cooling curve is hindered by the presence of the cool ash plume masking the first few minutes of the cycle, thus we are unable to conclusively determine whether T_s is equal to the starting temperature of the surface for a particular cycle. Assuming that T_s is equal to the initial temperature, each cooling curve can then be fitted fairly well with exponential functions (Figure 1). Alternatively, if we remove the first ~3 minutes of each cycle to accommodate the lack of surface temperature data, a slightly better fit to the data can be obtained by quadratic expressions. We calculated the average cooling, excluding the initial ~3 minutes of each cycle, to be 0.9–1.6°C/min. This compares to 1.2–3°C/min calculated for the proximal section of the Santiaguito block lava flow [*Harris et al.*, 2002], and to 2.7°C/min calculated for basaltic pahoehoe surface by *Hon et al.* [1994] (taking into account only data beyond the first three minutes which represents the initial rapid cooling phase).

4. Radiance Spectra

[8] Three hundred radiance spectra were collected for a 15-minute period before the start of cooling cycle 1 and 290 were collected after the start of cycle 2 (Figure 1). The large number of wavebands available to the spectroradiometer allows us to collect radiant flux as a near-continuous spectrum from 0.4 to 2.5 μm. Where a number of thermal sources are present in the IFOV, an integrated radiance spectrum will be produced which can then be de-convoluted to provide an estimate of the temperature and fractional area of each source [*Flynn et al.*, 1993]. For our dataset we applied a simple two-component mixing model developed by *Flynn et al.* [1993]. This model calculates a Planck curve that best fits the measured radiance spectrum by varying the temperatures of the hot component (T_h), cool component (T_c), as well as the area of the hot component (f_h). Temperatures for each component were allowed to vary from 0–950°C and fractional area from 0 to 1 for model calculations. We assume that 950°C is a reasonable maximum eruptive temperature based on previous values of 800–850°C from Fe-Ti oxides and optical pyrometer measurements and taking into account recent increase in SiO2 content by adding 100°C (W. I. Rose, personal communication, 2003). We refer the readers to *Flynn et al.* [1993] for complete treatment of the model used in this work.

[9] In Figure 3 we display three spectra from our collected dataset. Spectra A and B were collected during the first segment and spectrum C was collected during the second segment. Two atmospheric absorption bands at 1.3–1.5 μm and 1.8–2.0 μm are evident by the decrease in radiant flux at those wavebands. Very small amount of radiant flux detected for both spectra A and C at 0.9–1.3 μm indicate the presence of high temperature radiative component in the IFOV. The notable increase in radiance flux at the same wavelengths for spectrum B suggests an increase in the fractional area of the high temperature radiator. More significant changes in flux for the three spectra occur at the wavelength ranges of 1.5–2.5 μm, varying from low (spectrum A), to high (spectrum B) and to intermediate (spectrum C). Changes in the overall slope of the spectral curve suggest changes in temperature and fractional areas of each component, which can be elucidated by applying the mixing model to these spectra. For spectrum A, we obtain T_c = 187°C, T_h = 947°C and $f_h = 2.59 \times 10^{-05}$, which is consistent with a surface composed of a fairly cool crust with rare fractures radiating at or near magmatic temperature. For spectrum B, T_c = 467°C, T_h = 468°C and f_h = 0.39, which suggests an isothermal surface. Solution for spectrum C also yields an isothermal surface with T_c = 355°C, T_h = 359°C and f_h = 0.54.

[10] Applying the model on the rest of the dataset illustrates how the two solutions for spectrum A and C represent a fundamental difference between the two segments of the spectral dataset (Figure 4). The two-component structure is consistent throughout most of the first segment,

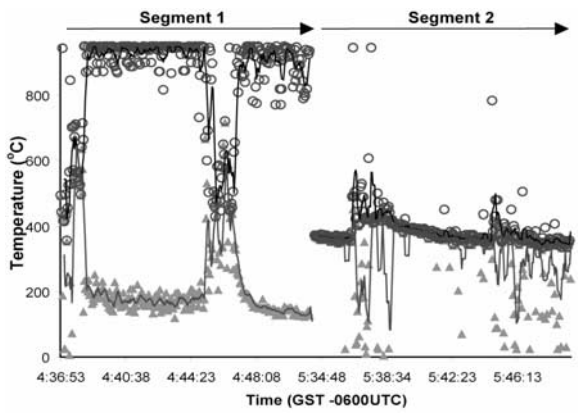

Figure 4. Temperature values derived from radiance flux dataset showing two-component thermal surface for segment 1 and homogeneous surface for segment 2. T_h is shown in solid circles and T_c is shown in gray solid triangles. 15s moving average for T_h and T_c are shown in solid black and gray solid lines respectively.

with T_c at temperatures of 120–250°C cooling with time while T_h approximates 850–950°C. The f_h values remain extremely small (<0.02%). This suggests that, at this stage, the surface is comprised of an extensive blocky crust that is cooling slowly with time, with localized fractures radiating at high temperature T_h, possibly due to heat escaping from hotter underlying material. Conversely, the 2nd segment is characterized by an isothermal surface for nearly the entire duration of the segment. Almost all of the solutions for T_c and T_h fall within 6°C of one another in this segment. There is a significant increase in temperature of the dominant radiating component from the previous segment, with temperatures ranging from 350 to 500°C during the second segment, compared to 120–250°C during the first segment.

[11] Departures from the two-component structure for the 1st segment, represented by radiance spectrum C, occurred at the beginning and towards the middle of the segment. Neither of these events is registered in the IR thermometer data and no video footage is available for visual confirmation of the actual activity responsible for the events. These events are characterized by rapid convergence of T_c and T_h to an intermediate value (400–600°C) and after ~3 minutes all parameters returned to their pre-event trends. This suggests the rapid development and decay of an isothermal surface. Such an event may be similar to the thermally indistinct ash/gas venting events observed from video footage. The rapid recovery to the overall cooling trend is consistent with cooling of a surface composed of fine particles that reached thermal equilibrium with the underlying surface in a short period of time.

[12] The spectra-derived crust temperature appears to be 50–200°C higher than the IR thermometer measurements. We explain this discrepancy partly as a result of having slightly different IFOVs for the two instruments, where the IR thermometer may be viewing part of the dome that is relatively cooler in temperature, as well as to the differential emissivity and atmospheric effects at the different operational wavebands of the two instruments.

5. Discussion

[13] The combined use of IR thermometer, spectroradiometer and video footage at high data collection frequencies (0.3 Hz) have allowed us to document and characterize at-vent cooling cycles and changes in the thermal state and morphology of the surface at Santiaguito. Using the IR thermometer dataset and video observations, we recognize that each cooling cycle is initiated and terminated by a thermal resurfacing event which is temporally synchronous with the periodic ash eruptions. Not all of the ash eruptions result in resurfacing, at least not of the dome sector observed. The results of temperature retrievals from spectral radiance datasets confirm that during thermal resurfacing events, the observed surface morphology was transformed from a two-component crust-crack surface to an isothermal surface at an intermediate temperature. Thereafter cooling dominates as the isothermal surface cools by radiation and convection to generate a logarithmically decaying cooling curve. The low temperatures registered by the ash plumes coupled with the absence of nighttime visual observations of incandescent ejecta eliminate plume fallout as a source of the thermal resurfacing.

[14] From the video data we recognize a progressive decrease in relative intensity of subsequent ash eruptions in each cycle. These tend not to be associated with thermal renewal. We thus assume that only ash eruptions beyond a certain intensity threshold that can cause the change in thermal state of the observed surface, and/or smaller events only affect localized areas beyond the considered measurement area. We propose that ash eruptions of sufficient energy and intensity can cause the change in the thermal state of the surface by creating more fractures or widening the fractures on the surface crust, and/or stirring or rotating the lava blocks on the surface. These processes expose surfaces for which cooling has been retarded due to insulation by an overlying crust. The relatively low temperatures of these surfaces show that, although elevated, they are at intermediate temperatures lower than that for dacitic lava, and thus do not represent exposure/emplacement of fresh lava.

[15] The implication for satellite monitoring of volcanoes is significant in that despite its low-level background temperature, at-vent activities at Santiaguito should be detectable the near-IR as well as the thermal IR wavelengths due to the periodic thermal resurfacing. This observation is consistent with the analysis of *Harris et al.* [2002] where the vent appears thermally anomalous in TM data but the crust-dominated block flow does not. Our results suggest that the lava dome surface can be modeled with a two-component surface (chilled crust broken by hot cracks). However, given the very small fractional area of the hot component, and the presence of isothermal crust, a single cool crust component may well be sufficient. This in turn facilitates the use of satellite data sets to extend our observations beyond the temporal limits of field-based campaigns to reveal hour-to-day long as well as long-term temperature variations and activity cycles. The analysis of the automated thermal alert information using GOES or MODIS data [*Harris et al.*, 2001; *Wright et al.*, 2004] with their 15 minute to 6 hr temporal resolutions would provide a complementary long-term thermal data set to examine cyclic behavior of Santiaguito for week-to-month long time scales. Both data sets could be used to provide constraints for models that simulate cyclic conduit dynamics, rheological changes and pressurization cycles [e.g., *Denlinger and Hoblitt*, 1999; *Barmin et al.*, 2002].

[16] **Acknowledgments.** Funding for this work is from NASA Grant NCC 5-461 & NGT5-40076, NASA Pathfinder Grant 59413, and NASA ESS Fellowship. We would like to thank CONRED, INSIVUMEH, R. Wolf, J. Byman and S. Carn for field support. This is SOEST contribution #6483 and HIGP contribution #1349.

References

Barmin, A., O. Melnik, and R. S. J. Sparks (2002), Periodic behavior in lava dome eruptions, *Earth Planet Sci. Lett.*, *199*, 173–184.

Bluth, G. J., Y. K. Branan, W. I. Rose, and O. Matias (2002), Observations of Santiagutio's eruptive and passive emissions, *Eos Trans. AGU*, *83*(47), Fall Meet. Suppl., Abstract V72C-03.

Denlinger, R. P., and R. P. Hoblitt (1999), Cyclic eruptive behavior of silicic volcanoes, *Geology*, *27*, 459–462.

Flynn, L. P., P. J. Mouginis-Mark, J. C. Gradie, and P. G. Lucey (1993), Radiative temperature measurements at Kupaianaha lava lake, Kilauea volcano, Hawaii, *J. Geophys. Res.*, *98*, 6461–6476.

Harris, A. J. L., E. Pilger, L. P. Flynn et al. (2001), Automated, high temporal resolution, thermal analysis of Kilauea volcano, Hawaii, using GOES-9 satellite data, *Int. J. Remote Sens.*, *22*, 945–967.

Harris, A. J. L., L. P. Flynn, O. Matias, and W. I. Rose (2002), The thermal stealth flows of Santiaguito Dome, Guatemala: Implications for the cooling and emplacement of dacitic block-lava flows, *Geol. Soc. Am. Bull.*, *114*, 533–546.

Hon, K., J. Kauahikaua, R. Denlinger, and K. Macakay (1994), Emplacement and inflation of pahoehoe sheet flows: Observations and measurements of active lava flows on Kilauea Volcano, Hawaii, *Geol. Soc. Am. Bull.*, *106*, 351–370.

Oppenheimer, C. (1993), Thermal distributions of hot volcanic surfaces constrained using three infrared bands of remote sensing data, *Geophys. Res. Lett.*, *20*, 431–434.

Rose, W. I. (1987), Volcanic activity at Santiaguito volcano, 1976–1984, *Spec. Pap. Geol. Soc. Am.*, *212*, 17–27.

Rothery, D. A., P. W. Francis, and C. A. Wood (1998), Volcano monitoring using short wavelength infrared data from satellites, *J. Geophys. Res.*, *93*, 7993–8008.

Wooster, M. J., T. Kaneko, S. Nakada, and H. Shimizu (2000), Discrimination of lava dome activity styles using satellite-derived thermal structures, *J. Volcanol. Geotherm. Res.*, *102*, 97–118.

Wright, R., L. P. Flynn, H. Garbeil et al. (2004), MODVOLC: Near-real-time thermal monitoring of global volcanism, *J. Volcanol. Geotherm. Res.*, *135*, 29–49.

G. J. Bluth and W. I. Rose, Department of Geological Engineering, Geology and Geophysics, MTU, Houghton, MI 49931, USA.

L. P. Flynn, A. J. L. Harris, and S. T. M. Sahetapy-Engel, HIGP/SOEST, University of Hawai'i, Honolulu, HI 96822, USA. (sahetapy@higp.hawaii.edu)

O. Matias, INSIVUMEH, 7a Av. 14-57, Zona 13, Guatemala City, Guatemala.